

Effect of Molecular Structure on Wetting Behavior at the Air–Liquid Interface of Water + Alcohol Mixtures

Ming-Chih Yeh, Ping-Chang Lin, and Li-Jen Chen*

Department of Chemical Engineering, National Taiwan University, Taipei, Taiwan 10617, Republic of China

Received: December 31, 2003; In Final Form: April 22, 2004

In this study, the wetting behavior of binary water + alcohol mixtures was carefully investigated by using eight different short-chain alcohols. These binary mixtures exhibit liquid–liquid equilibrium over the experimental temperature range 10–40 °C. The wetting behavior of the upper liquid (alcohol-rich) phase at the surface of the lower liquid (aqueous) phase can be determined according to the wetting coefficient resulting from the interfacial tension measurements. Molecular structure of alcohols plays an essential role in the wetting behavior. The purpose of this study is threefold. (1) The effect of the hydrocarbon chain length of alcohols was examined by employing water + 1-butanol (C₄E₀), water + 1-pentanol (C₅E₀), and water + 1-hexanol (C₆E₀) three systems, where C_iE_j is the abbreviation of a nonionic polyoxyethylene alcohol C_iH_{2i+1}(OCH₂-CH₂)_jOH. The shorter chain alcohol has a stronger tendency to wet the surface of the aqueous phase. (2) The effect of number of oxyethylene groups of alcohols was investigated by using three mixtures, water + C₆E₀, water + C₆E₁, and water + C₆E₂. An interfacial phase transition from partial wetting to nonwetting was observed for water + C₆E_j mixtures as the number of oxyethylene groups *j* increases from 1 to 2. (3) The effect of isomeric structures of alcohols on wetting behavior was investigated by studying three mixtures, water + 1-pentanol, water + 2-pentanol (2-C₅E₀), and water + *tert*-pentanol (*t*-C₅E₀). An interfacial phase transition from partial wetting to complete wetting occurs while the molecular structure of alcohols evolves from linear (C₅E₀) to near spherical (*t*-C₅E₀) shape.

Introduction

Three fluid phases, α , β , and γ , are in equilibrium under gravity and the densities of these three phases are in the order $\rho_\alpha > \rho_\beta > \rho_\gamma$, as shown in Figure 1a. The wetting behavior of the middle β phase can be easily realized by the wetting coefficient defined as $W = (\sigma_{\beta\gamma} - \sigma_{\alpha\gamma})/\sigma_{\alpha\beta}$ and the contact angle θ spanned by the α – β and the β – γ interfaces, as shown in Figure 1b. The symbol σ_{ij} stands for the interfacial tension of the interface separating *i* and *j* phases. On the basis of the wetting coefficient and the contact angle, the wetting behavior can then be classified into four types, as illustrated in Figure 2.

(a) $W = -1$ and $\theta = 0^\circ$, a complete wetting β phase at the α – γ interface, as shown in Figure 2a. In this case, the tensions obey the Antonow's rule,¹ $\sigma_{\alpha\gamma} = \sigma_{\alpha\beta} + \sigma_{\beta\gamma}$.

(b) $-1 < W < 0$ and $0^\circ < \theta < 90^\circ$, a partial wetting β phase at the α – γ interface, as shown in Figure 2b. The relationship between tensions is $\sigma_{\alpha\gamma} < \sigma_{\alpha\beta} + \sigma_{\beta\gamma}$, with $\sigma_{\alpha\gamma} > \sigma_{\beta\gamma}$.

(c) $0 < W < 1$ and $90^\circ < \theta < 180^\circ$, a partial wetting β phase at the α – γ interface, as shown in Figure 2c. In this condition, a partial wetting α phase also exists at the β – γ interface. The relationship between tensions is $\sigma_{\beta\gamma} < \sigma_{\alpha\beta} + \sigma_{\alpha\gamma}$ with $\sigma_{\alpha\gamma} < \sigma_{\beta\gamma}$.

(d) $W = 1$ and $\theta = 180^\circ$, a nonwetting β phase at the α – γ interface, as shown in Figure 2d. While the system has a substantial amount of the β phase, the α phase would exhibit complete wetting behavior at the β – γ interface, as shown in Figure 2d'. In this situation, the Antonow's rule is applied in the form $\sigma_{\beta\gamma} = \sigma_{\alpha\beta} + \sigma_{\alpha\gamma}$.

In the last two decades, the wetting behavior of ternary water + oil + C_iE_j mixtures had been extensively and systematically

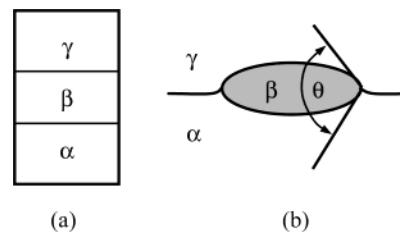


Figure 1. (a) Schematic illustration of a three-fluid-phase α , β , and γ coexisting system in equilibrium under the gravity. (b) Definition of contact angle θ in a three-fluid-phase-coexisting system.

studied.^{2–10} Numerous experimental approaches including direct eye observation,^{3,10} contact angle measurement,^{5,6,8} interfacial tension measurement,^{4,6,8–10} and ellipsometry¹¹ were employed to investigate the adsorption and wetting behavior of the middle amphiphile-rich phase at the oil–water interface. It was found that these ternary systems can exhibit diverse wetting behaviors by simply varying thermodynamic variables, such as temperature,^{3,5–8} oil hydrocarbon chain length,^{7,9,10} amphiphilicity of an amphiphile,⁵ and salinity.^{12,13} The most intriguing phenomenon is observed for the water + tetradecane + C₆E₂ system⁶ in that the middle C₆E₂-rich phase would undergo an interfacial phase transition from nonwetting to partial wetting to complete wetting along with increasing temperature. This observation confirms the suggestion that the wetting behavior can be related to the temperature dependence of amphiphilicity of an amphiphile.²

On the other hand, the binary water + C_iE_j systems are also rich in wetting behavior although these systems are relatively simple. Donahue and Bartell¹⁴ had reported the surface/interfacial tensions of several binary water + organic liquid mixtures, including some short- and medium-chain alcohols

* Corresponding author. E-mail address: ljchen@ccms.ntu.edu.tw.

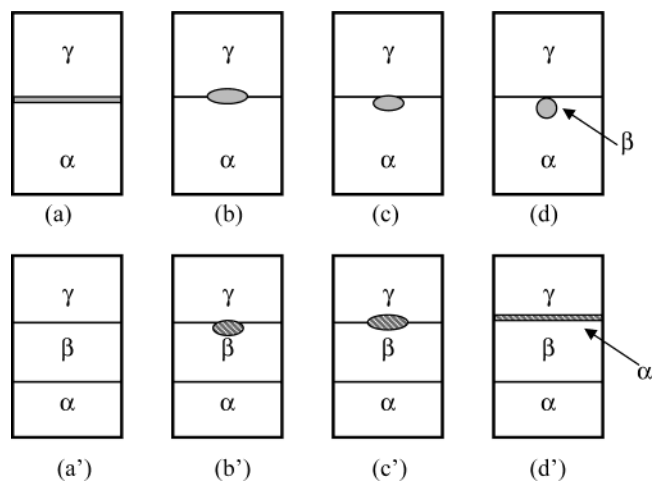


Figure 2. Wetting behavior at a fluid–fluid interface. (a) A complete wetting β phase at α – γ interface, (b) a partial wetting β phase at α – γ interface, (b') a partial wetting α phase at β – γ interface, (c) a partial wetting β phase at α – γ interface, (c') a partial wetting α phase at β – γ interface, (d) a nonwetting β phase at α – γ interface, (d') a complete wetting α phase at β – γ interface. The expected condition for only a small amount of the β phase at the α – γ interface is shown in the upper row and the condition for a substantial amount of the β phase is shown in the lower row.

(C_iE_0), only at 298.15 K. The interfacial tensions were related to the reciprocal solubilities and were used to determine the wetting behavior. It was found that the alcohol-rich phase exhibits partial wetting behavior at the air–water interface. It is believed that the surface tension of the aqueous phase is substantially lowered by the adsorbed alcohol molecules that prevent the spreading of the alcohol-rich phase over the water surface.

The wetting behavior of the water + C_8E_j homologues mixtures at 298.15 K was investigated by Kahlweit and Busse.² With increasing the number of oxyethylene groups j from 0 to 3 stepwise, the wetting coefficient evolves from -0.3 for C_8E_0 to >0 for C_8E_2 and C_8E_3 , indicating a tendency of the occurrence of an interfacial phase transition from partial wetting to nonwetting. It is well understood that the system water + C_iE_j with a larger j at a fixed i has a higher lower critical solution temperature (LCST).¹⁵ Hence, an increase in j at a constant temperature is equivalent to bringing the system closer to its LCST. Accordingly, these authors suggested that a wetting transition for the C_8E_j -rich phase from partial wetting to nonwetting at the surface of the aqueous phase should occur along with increasing j on the basis of the critical point wetting theory.¹⁶ Hirtz et al.¹¹ had applied ellipsometry to investigate the effect of the molecular shape anisotropy on the wetting and adsorption behavior in binary water + amphiphile systems. Aratono et al.^{17,18} had systematically studied the temperature dependence of surface and interfacial tensions of water + long-chain alcohols ($i = 8$ –12). The crossover between surface tensions of both liquid phases and the intruding phenomena of the aqueous phase at the air–alcohol interface were demonstrated. The interfacial phase transitions between the expanded and the condensed states were also manifested.

In this work, several alcohols C_iE_0 and polyoxyethylene alcohols C_iE_j were employed to verify the connection of the molecular structure of alcohol with the wetting behavior of the alcohol-rich phase at the interface separating air and the aqueous phase. This paper is organized as follows. The experimental details are given in the next section. The experimental results of surface/interfacial tensions for eight binary mixtures are presented and then the molecular structure effect on the wetting

behavior is discussed. Finally, this study is concluded in the last section by demonstrating the wetting behavior in a ternary water + C_6E_2 + t - C_5E_0 mixture.

Experimental Section

1-Butanol ($>99.5\%$) was purchased from Riedel-de Haën. 1-Pentanol ($>98.5\%$), 2-pentanol ($>98\%$), 2-methyl-2-butanol ($>99.5\%$), 1-hexanol ($>98\%$), and diethylene glycol monoethyl ether (C_6E_2) of 98% purity were products of Merck Chemical. Ethylene glycol monoethyl ether (C_6E_1) and ethylene glycol monomethyl ether (C_5E_1) were obtained from Bachem AG. Four chemicals, 1-pentanol, 2-pentanol, 1-hexanol, and C_6E_2 , were fractionally distilled under reduced pressure until a purity of $>99.5\%$, as determined by gas chromatography, was attained. Water was purified by reverse osmosis (Millipore, Milli-RO Plus 10) followed by a Milli-Q (Millipore) purification system with the resistivity always better than $18.2 \text{ M}\Omega\text{-cm}$.

The mixture was prepared in a flask and placed in a water bath for at least several hours or for sometimes up to several days to allow the system to reach equilibrium. The temperature stability of the water bath was better than $\pm 0.005 \text{ K}$. Before and during the equilibration process, the samples were shaken vigorously several times to ensure thorough mixing. After equilibrium was reached, both phases were transparent with sharp, mirrorlike interfaces. Following equilibration, both phases were carefully transferred by using a pipet and put into a quartz cell of $26 \times 41 \times 43 \text{ mm}$ inside dimensions for the tension measurement. This quartz cell along with a cover was housed in a double-walled Pyrex vessel thermostated by means of circulating water. The double-walled Pyrex vessel was placed in an air thermostat chamber, which was made from acrylic material, to eliminate the effect of the environmental temperature fluctuation on the temperature stability of the sample. The temperature stability of the liquid in the quartz cell was better than $\pm 0.1 \text{ K}$.

A homemade pendant drop/bubble tensiometer was used to measure the surface tensions of both liquid phases against air and the interfacial tension between two coexisting liquid phases. The details of the setup are described elsewhere.¹⁹

Results and Discussion

In this study, the surface/interfacial tensions were performed for eight binary mixtures: water + C_4E_0 , water + C_5E_0 , water + 2- C_5E_0 , water + t - C_5E_0 , water + C_5E_1 , water + C_6E_0 , water + C_6E_1 , and water + C_6E_2 . All these binary mixtures exhibit liquid–liquid equilibrium over the temperature range 10 – $40 \text{ }^\circ\text{C}$ at the normal pressure,^{20–23} except the system water + C_6E_2 . The LCST of the system water + C_6E_2 is $10.79 \text{ }^\circ\text{C}$,²³ slightly higher than $10 \text{ }^\circ\text{C}$. The wetting coefficient is determined by the surface/interfacial tensions. The wetting behavior of the alcohol-rich phase at the interface separating air and the aqueous phase is then verified according to the wetting coefficient, as mentioned above.

The Effect of Alcohol Chain Length on the Wetting Behavior. The surface/interfacial tensions of water + 1-butanol (C_4E_0), water + 1-pentanol (C_5E_0), and water + 1-hexanol (C_6E_0) systems were measured and employed to examine the effect of alcohol chain length on the wetting behavior of the alcohol-rich phase at the surface of the aqueous phase. Figure 3 shows the experimental results of the surface/interfacial tensions as a function of temperature for three water + C_iE_0 systems. The literature data of the surface/interfacial tensions by Donahue and Bartell¹⁴ and by Villers and Platten²⁴ are also shown as open symbols and dashed lines, respectively, in Figure

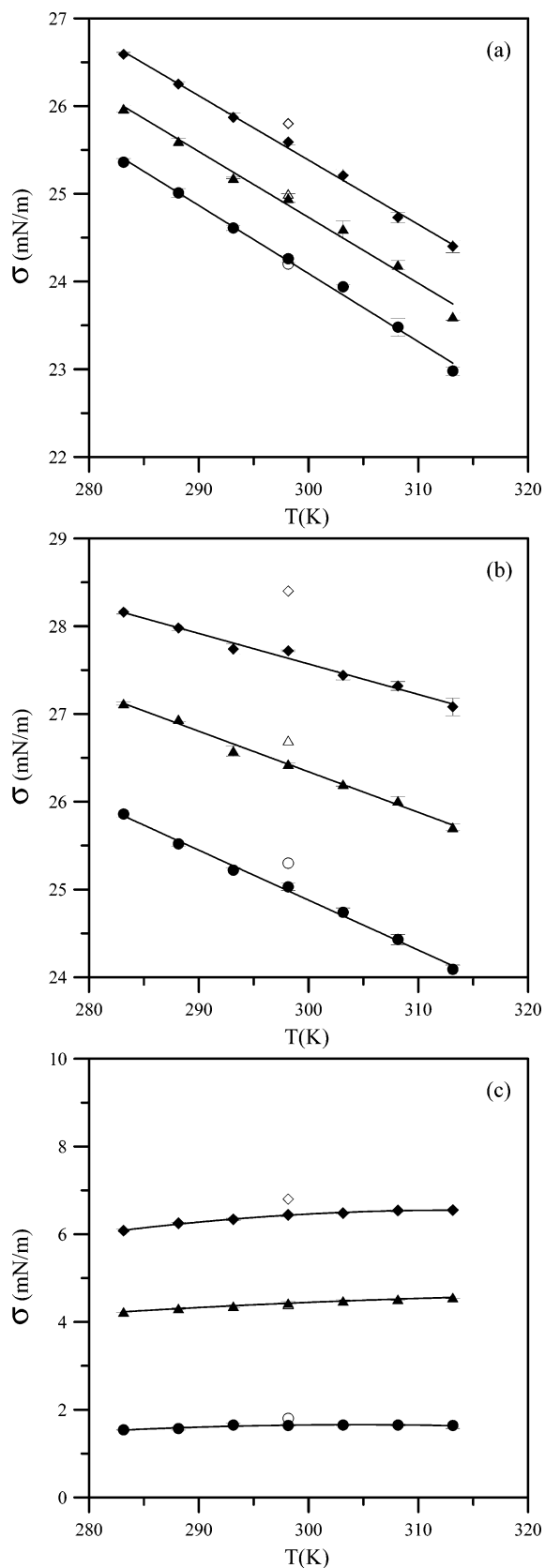


Figure 3. Variation of tensions as a function of temperature for three water + C_iE_0 systems: (a) $\sigma_{\beta\gamma}$, the air–alcohol-rich interface; (b) $\sigma_{\alpha\gamma}$, the air–aqueous interface; and (c) $\sigma_{\alpha\beta}$, the alcohol-rich–aqueous interface. C_4E_0 (●,○); C_5E_0 (▲,△); C_6E_0 (◆,◇). Filled symbols (this work); open symbols (ref 14); dashed lines (ref 24).

3 for comparison. It is believed that the discrepancy between these results is due to different experimental approaches and the purities of chemicals. Donahue and Bartell¹⁴ also employed

pendant drop method; however, the images were acquired by taking photographs. In this study, a more precise digital image processing method was applied. On the other hand, Wilhelmy plate method was used by Viller and Platten²⁴ and no information about chemicals is reported.

Figure 3a shows that the surface tension of the alcohol-rich phase $\sigma_{\beta\gamma}$ decreases along with increasing temperature and with decreasing alcohol chain length. These trends are similar to those observed for the surface tensions of pure alcohols. Aratono et al.¹⁷ pointed out that the longer chain alcohols interact more strongly than the shorter ones in the alcohol-rich phase. Hence, the transfer of alcohol molecules from the bulk phase to the surface of the alcohol-rich phase, to reduce the surface energy, is energetically less favorable for the longer chain alcohols. Variations of the surface tension of the aqueous phase $\sigma_{\alpha\gamma}$ as a function of temperature and alcohol chain length, shown in Figure 3b, are similar to that of the C_iE_0 -rich phase, indicating that the shorter chain alcohol possesses better surface activity at the interface separating air and the aqueous phase. Figure 3c illustrates that the interfacial tension $\sigma_{\alpha\beta}$ increases with increasing alcohol chain length. Contrary to short-chain alcohol systems ($i = 4-6$), for long-chain alcohol systems ($i = 8-12$), both $\sigma_{\alpha\gamma}$ and $\sigma_{\alpha\beta}$ decrease with increasing alcohol chain length. Toyomasu et al.¹⁸ suggested that both the formations of the α - β and α - γ interfaces are dominated by the orientation of hydrocarbon chains and the energetically favorable interaction between hydrocarbon chains. Hence, this interesting crossover behavior can be considered as the outcome of the delicate balance between the mutual solubility in the bulk phases and the surface activity of the alcohol at the interface.

For the short-chain alcohol systems ($i = 4-6$), the mutual solubility in the bulk phases increases substantially with decreasing alcohol chain length, which makes the difference between two bulk phases (the aqueous phase and the alcohol-rich phase) become smaller for the system of a shorter chain alcohol. As a consequence, both $\sigma_{\alpha\gamma}$ and $\sigma_{\alpha\beta}$ decrease with decreasing alcohol chain length. On the other hand, for the long-chain alcohol systems ($i = 8-12$),¹⁸ the surface activity of the alcohol at the interface plays an essential role in the interfacial tensions. The alcohols can be considered as “simple” amphiphilic compounds. However, the amphiphilicity of alcohols becomes dramatically pronounced when the alcohol chain length is increased, especially when $i > 10$. As one can see in Figure 4 of ref 18, both $\sigma_{\alpha\gamma}$ and $\sigma_{\alpha\beta}$ decrease substantially with increasing alcohol chain length, that is, the surface activity of the alcohol enhances as the alcohol chain length increases from C_8E_0 to $C_{12}E_0$.

Figure 4 shows the wetting coefficients as a function of temperature for three water + C_iE_0 systems ($i = 4-6$). The wetting coefficient decreases with increasing temperature and with decreasing alcohol chain length. This infers that the alcohol-rich phase may completely wet the air–water interface at higher temperatures or for alcohols of shorter chain. However, all alcohols shorter than C_4E_0 are completely miscible with water at normal pressure. For long-chain alcohols ($i = 8, 10, 11$, and 12), the wetting behavior has already been determined^{17,18} on the basis of tension measurements. At 293.15 K, the alcohol-rich phase exhibits the type b, shown in Figure 2, wetting behavior ($\theta < 90^\circ$) for water + C_8E_0 system and then transitions to the type c wetting behavior ($90^\circ < \theta < 180^\circ$) for water + $C_{10}E_0$ and water + $C_{11}E_0$ systems. This suggests that for water + C_iE_0 systems, the wetting behavior is dominated by the orientation of hydrocarbon chains at the air–water interface. The short alcohol molecules show usual surface activity and

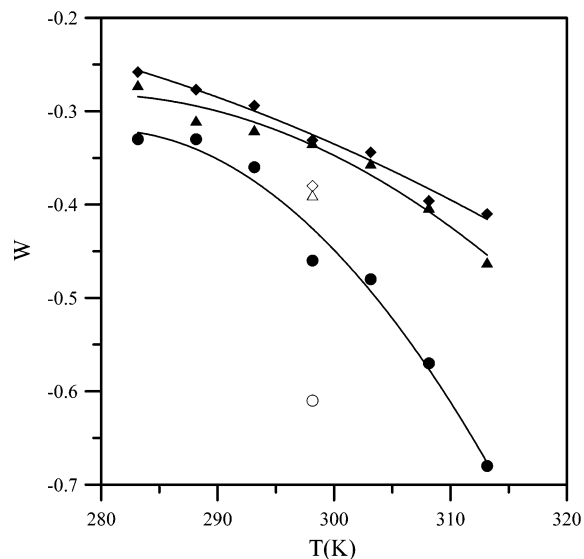


Figure 4. Variation of wetting coefficients as a function of temperature. C_4E_0 (●,○, solid curve); C_5E_0 (▲,△, dashed curve); C_6E_0 (◆,◇, solid curve). Filled symbols (this work); open symbols (ref 14).

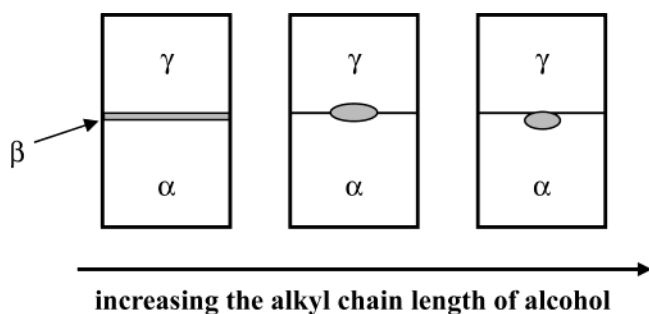


Figure 5. Evolution of the wetting behavior of the alcohol-rich phase at the interface separating air and the aqueous phase in the two-liquid-phase-coexisting region as a function of the alkyl chain length of an alcohol.

tend to spread over the surface of the aqueous phase. When the alcohol chain length increases, the strong interaction between alkyl chains repels the alcohol lens downward, as illustrated in Figure 2c, that is, the contact angle θ increases when the alcohol chain length increases, as well as the wetting coefficient. In other words, the wetting behavior of the alcohol-rich phase has a tendency to completely wet the air–water interface when the alcohol chain length decreases at a fixed temperature. To summarize the experimental evidences, the evolution of wetting behavior of water + C_iE_j systems as a function of alkyl chain length of an alcohol can be generally described in Figure 5.

The Effect of Isomeric Structure of Alcohols on the Wetting Behavior. Three isomeric alcohols, 1-pentanol (C_5E_0), 2-pentanol ($2-C_5E_0$), and 2-methyl-2-butanol ($t-C_5E_0$), were chosen to study the effect of the molecular structure on the wetting behaviors. In addition, the water + C_5E_1 system was also included to examine the influence of an additional hydrophilic oxyethylene group on the wetting behavior.

Figure 6 illustrates the temperature dependence of the surface/interfacial tensions for these four water + C_5E_j systems. The surface tensions of the alcohol-rich phase $\sigma_{\beta\gamma}$ are shown in Figure 6a. At any temperature, the $\sigma_{\beta\gamma}$'s for three isomer systems are in the order $\sigma_{\beta\gamma}(C_5E_0) > \sigma_{\beta\gamma}(2-C_5E_0) > \sigma_{\beta\gamma}(t-C_5E_0)$. That implies that $\sigma_{\beta\gamma}$ is predominated by the interaction between hydrophobic alkyl chains. It was suggested^{17,18} that the longer hydrocarbon chains interact more strongly than the shorter ones in the alcohol-rich phase, and the transfer of alcohol molecules

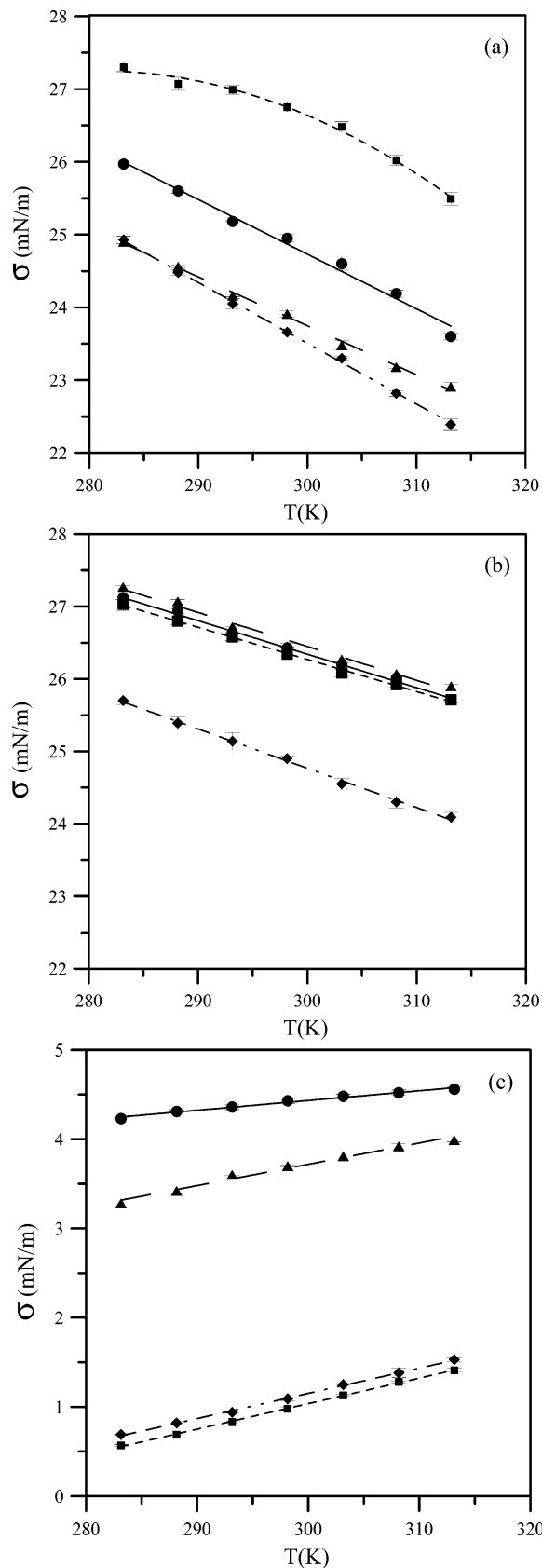


Figure 6. Variation of tensions as a function of temperature for four water + C_5E_j systems: (a) $\sigma_{\beta\gamma}$, the air–alcohol-rich interface; (b) $\sigma_{\alpha\gamma}$, the air–aqueous interface; and (c) $\sigma_{\alpha\beta}$, the alcohol-rich–aqueous interface. C_5E_0 (●, solid curves); $2-C_5E_0$ (▲, long-dashed curves); $t-C_5E_0$ (◆, dashed–dotted curves); C_5E_1 (■, dashed curves).

from bulk phase to the air–liquid interface is energetically unfavorable for longer chain alcohols. Thus, the near globular

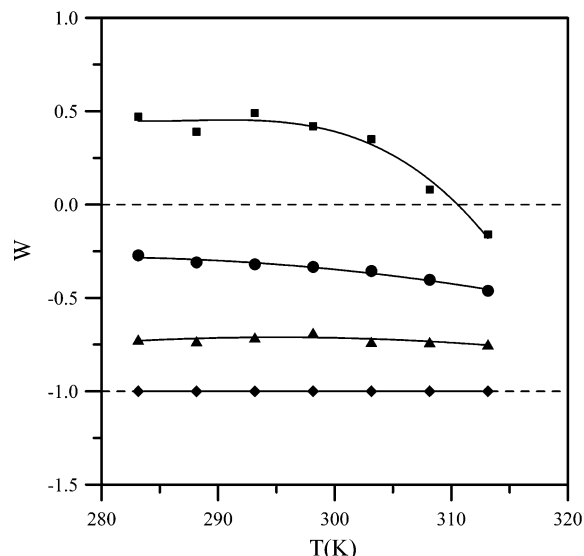


Figure 7. Variation of wetting coefficients as a function of temperature. C₅E₀ (●); 2-C₅E₀ (▲); *t*-C₅E₀ (◆); C₅E₁ (■).

molecule, such as *t*-C₅E₀, provides lower surface tension because of its shorter “effective” chain length. The effective chain length stands for the linear hydrocarbon chain length along the hydroxyl group. For the water + C₅E₁ system, the hydrophilicity of oxyethylene groups enhances the interactions between C₅E₁ and water in the bulk C₅E₁-rich phase. Consequently, the surface tension $\sigma_{\beta\gamma}$ of the water + C₅E₁ system is the largest among these four water + C₅E_j systems. In addition, the surface tension $\sigma_{\beta\gamma}$ decreases as the effective chain length decreases from the primary alcohol (C₅E₀), the secondary alcohol (2-C₅E₀), and further to the tertiary alcohol (*t*-C₅E₀).

In general, the surface tension of the aqueous phase $\sigma_{\alpha\gamma}$ is expected to reflect the surface activity of the alcohol. Figure 6b demonstrates that the surface activity is comparable for three components C₅E₀, 2-C₅E₀, and C₅E₁. On the other hand, the near globular shape molecule *t*-C₅E₀ has a relatively low $\sigma_{\alpha\gamma}$. That indicates that the *t*-C₅E₀ molecule favors to adsorb at the air–water interface. On the contrary, the straight-chain molecules tend to form a well-structured adsorption layer at the interface and prevent further adsorption to lower the surface tension.

Figure 6c illustrates the variation of the interfacial tension $\sigma_{\alpha\beta}$ as a function of temperature. The tensions for two mixtures, water + *t*-C₅E₀ and water + C₅E₁, are substantially lower than that for the other two mixtures. There is a consistent picture that both *t*-C₅E₀ and C₅E₁ are more hydrophilic than the other two compounds C₅E₀ and 2-C₅E₀.

Figure 7 shows the wetting coefficient as a function of temperature for the four water + C₅E_j systems. The wetting coefficient falls into the range -0.3 and -0.5 for the system containing C₅E₀ and between -0.7 and -0.8 for the system containing 2-C₅E₀. The wetting coefficient remains equal to -1 over the experimental temperature ranging from 10 °C to 40 °C, that is, the *t*-C₅E₀-rich phase would completely wet the air–water interface. Conclusively, for the water + isomeric alcohol systems, a wetting transition from partial to complete wetting can be observed as the location of the hydroxyl group alters from primary (C₅E₀), secondary (2-C₅E₀), to tertiary (*t*-C₅E₀) carbon position. That is, the contact angle θ decreases when the effective chain length of alcohol decreases, as well as the wetting coefficient. In other words, the wetting behavior of the alcohol-rich phase has a tendency to completely wet the air–water interface when the effective chain length of alcohol

decreases at a fixed temperature. This observation is consistent with the finding in the previous section. Therefore, the evolution of wetting behavior of water + C_iE_j systems as a function of effective alkyl chain length of an alcohol can also be generally described in Figure 5.

The wetting coefficient for the water + C₅E₁ system is positive at low temperatures and drops to a negative value at 40 °C. Either adding an oxyethylene group or decreasing the alkyl chain length enhances the hydrophilicity of alcohol. However, both methods drive the wetting behavior to totally opposite directions. Adding an oxyethylene group to an alcohol would lead the system approaching nonwetting behavior. On the other hand, decreasing the alkyl chain length of an alcohol would drive the system approaching complete wetting behavior. In the next section, we will follow along this line to discuss the effect of adding oxyethylene groups to an alcohol on the wetting behavior.

The Effect of the Number of Oxyethylene Groups in an Alcohol on the Wetting Behavior. The homologues series of C₆E_j, C₆E₀, C₆E₁, and C₆E₂, was chosen to examine the influence of number of oxyethylene groups on the wetting behavior of water + C₆E_j mixtures. Figure 8 illustrates the temperature dependence of the surface/interfacial tensions for these three water + C₆E_j systems. The surface tensions of the alcohol-rich phase $\sigma_{\beta\gamma}$ for these three water + C₆E_j systems are in the order $\sigma_{\beta\gamma}(\text{C}_6\text{E}_2) > \sigma_{\beta\gamma}(\text{C}_6\text{E}_1) > \sigma_{\beta\gamma}(\text{C}_6\text{E}_0)$, as shown in Figure 8a. This implies that $\sigma_{\beta\gamma}$ is predominated by the interaction not only between hydrophobic alkyl chains but also between hydrophilic headgroups. Under the condition of a fixed hydrocarbon alkyl chain, the hydrophilic headgroup plays an essential role in determining the strength of the interface. The interaction between longer hydrophilic headgroups is stronger than that of the shorter ones in the alcohol-rich phase. Thus, the transfer of alcohol molecules from bulk phase to the interface is energetically unfavorable for alcohols with a longer hydrophilic headgroup. Thus, the less amphiphilic molecule, such as C₆E₀, provides a lower surface tension because of its weaker structured monolayer.

The surface tensions of the aqueous phase $\sigma_{\alpha\gamma}$ for these three water + C₆E_j systems are in the order $\sigma_{\alpha\gamma}(\text{C}_6\text{E}_0) > \sigma_{\alpha\gamma}(\text{C}_6\text{E}_2) > \sigma_{\alpha\gamma}(\text{C}_6\text{E}_1)$, as shown in Figure 8b. The compounds C₆E₁ and C₆E₂ are short-chain surfactants. Consequently, they can dramatically lower the surface tension $\sigma_{\alpha\gamma}$, as expected. However, the surface tension $\sigma_{\alpha\gamma}$ of the water + C₆E₂ system is higher than that of the water + C₆E₁ system. At liquid–liquid equilibrium, the surfactant concentration in the aqueous phase generally exceeds the critical micelle concentration (cmc). It is well understood that the surface is covered by a well-structured monolayer of surfactant when the surfactant concentration is above the cmc. The compound C₆E₂ has one more oxyethylene group than C₆E₁, which enhances the monolayer at water surface and is even more well-structured. As a consequence, $\sigma_{\alpha\gamma}(\text{C}_6\text{E}_2) > \sigma_{\alpha\gamma}(\text{C}_6\text{E}_1)$. This finding is consistent with our previous experiments on surfactants C₁₂E₄, C₁₂E₆, and C₁₂E₈. The surface tensions of the aqueous system for these three surfactants are in the order $\sigma_{\alpha\gamma}(\text{C}_{12}\text{E}_8) > \sigma_{\alpha\gamma}(\text{C}_{12}\text{E}_6) > \sigma_{\alpha\gamma}(\text{C}_{12}\text{E}_4)$ at a constant temperature when the surfactant concentration is above its cmc. Figure 8c shows that the interfacial tension $\sigma_{\alpha\beta}$ decreases, as expected, with increasing *j*.

The effect of the oxyethylene groups on the wetting coefficient is shown in Figure 9. The wetting coefficient increases with decreasing temperature and with increasing *j*, consistent with Kahlweit and Busse’s conjecture.² At a constant temper-

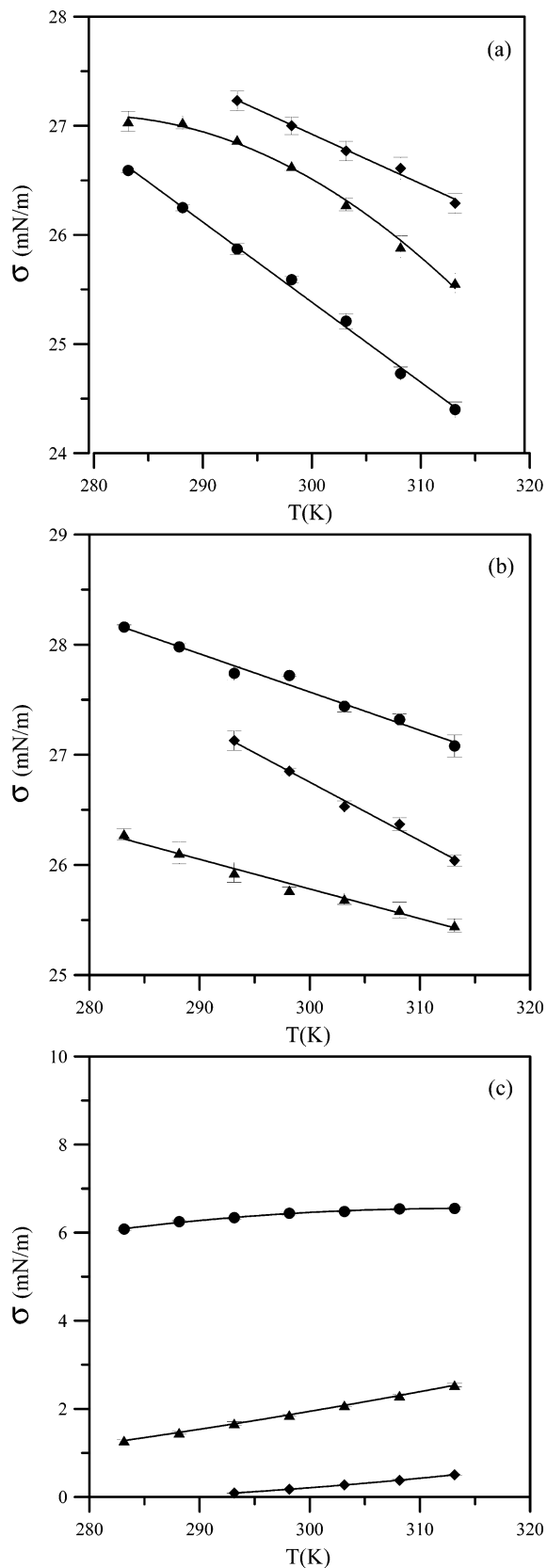


Figure 8. Variation of tensions as a function of temperature for three water + C_6E_j systems: (a) $\sigma_{\beta\gamma}$, (b) $\sigma_{\alpha\gamma}$, and (c) $\sigma_{\alpha\beta}$. C_6E_0 (●); C_6E_1 (▲); C_6E_2 (◆).

ature 298.15 K, the wetting coefficient evolves from -0.32 to 0.56 to 1 as the number of oxyethylene groups j increases stepwise from 0 to 2 . That is, a wetting transition from partial wetting to nonwetting is observed in the water + C_6E_j system

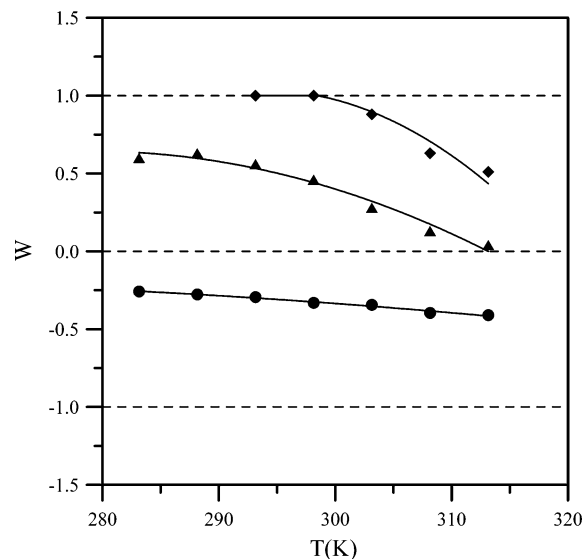


Figure 9. Variation of the wetting coefficient as a function of temperature. C_6E_0 (●); C_6E_1 (▲); C_6E_2 (◆).

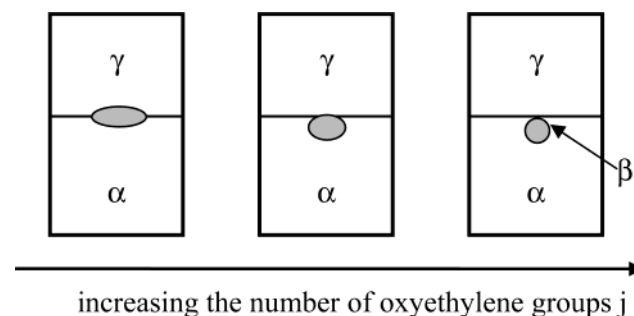


Figure 10. Evolution of the wetting behavior of the alcohol-rich phase at the interface separating air and the aqueous phase in the two-liquid-phase-coexisting region as a function of the number of oxyethylene groups.

by increasing the number of oxyethylene groups from 1 to 2 . In addition, for water + C_6E_2 mixture, a wetting transition from partial wetting to nonwetting occurs while the system approaches its LCST. This is the first observation to confirm the existence of a wetting transition from partial wetting to nonwetting while the binary water + C_iE_j system is brought close to its LCST.

Now, the wetting behavior of several other homologous series of binary water + C_iE_j systems is discussed. For the water + C_4E_j systems, when $j = 0$, the upper liquid phase exhibits partial wetting behavior of type b, as defined in Figure 2, as mentioned above. The nonwetting behavior of type d in Figure 2 had been demonstrated by Hirtz et al.¹¹ for the water + C_4E_1 system near its LCST. The compound C_4E_2 is completely miscible with water in all proportions at normal pressure. For the water + C_5E_j system, as mentioned in the previous section, the wetting behavior of the C_5E_j -rich phase changes from type b to type c when the system switches from water + C_5E_0 to water + C_5E_1 . For the water + C_6E_j systems, as mentioned above, the C_6E_j -rich phase undergoes interfacial phase transition: type b \rightarrow c \rightarrow d with increasing j . The water + C_8E_j systems² also show a similar trend in that type b wetting behavior is observed when $j = 0$ and 1 while type c wetting behavior is found when $j = 2$ and 3 . In other words, the contact angle θ increases when the number of oxyethylene groups increases, as well as the wetting coefficient. To sum up all these experimental evidences, the evolution of wetting behavior of water + C_iE_j systems as a function of number of oxyethylene groups j can be generally described in Figure 10.

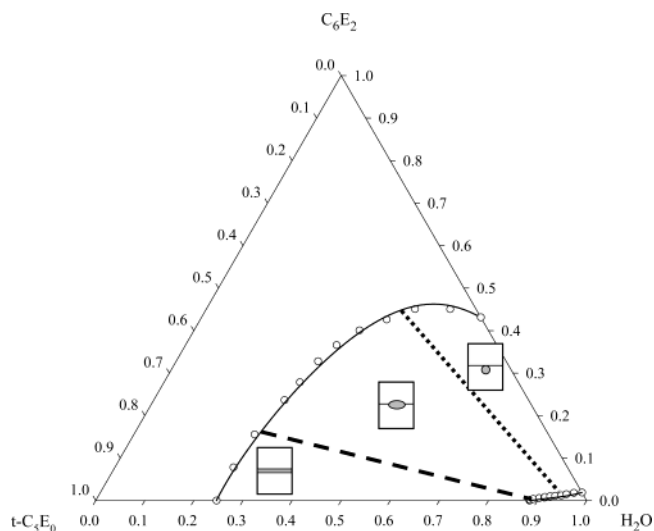


Figure 11. Phase²⁵ and wetting behavior of ternary water + *t*-C₅E₀ + C₆E₂ system at 293.15 K.

Conclusion

In this study, eight different binary water + C_{*i*}E_{*j*} systems are applied to examine the molecular structure effect on the wetting behavior of the C_{*i*}E_{*j*}-rich phase on the aqueous phase. Decreasing the alkyl chain length of an alcohol would drive the system approaching complete wetting behavior, as summarized in Figure 5. On the other hand, adding an oxyethylene group to an alcohol would lead the system approaching nonwetting behavior, as described in Figure 10. Both adding an oxyethylene group and decreasing the alkyl chain length would increase the hydrophilicity of alcohol and drive the wetting behavior of the alcohol-rich phase to totally opposite directions.

At 293.15 K, the alcohol-rich phase exhibits complete wetting behavior for the water + *t*-C₅E₀ system and nonwetting behavior for the water + C₆E₂ system. We now demonstrate the wetting behavior of the ternary water + C₆E₂ + *t*-C₅E₀ mixture as a concluding remark. Start with the binary water + C₆E₂ system and keep adding *t*-C₅E₀ into the system. First of all, we would observe a nonwetting droplet of the C₆E₂-rich phase suspending

at the interface separating air and the aqueous phase. With increasing the amount of *t*-C₅E₀, this nonwetting droplet would collapse and the partial wetting behavior is observed. With further adding *t*-C₅E₀, the partial wetting lens of the alcohol-rich phase would collapse to completely wet the interface. That is, a sequence of wetting transitions, nonwetting → partial wetting → complete wetting, would occur as the amount of *t*-C₅E₀ increases in the ternary system. Therefore, the two-liquid-phase-coexisting phase diagram is divided into three regimes according to the wetting behavior of the alcohol-rich phase, as summarized in Figure 11.

References and Notes

- (1) Antonow, G. N. *J. Chim. Phys.* **1907**, *5*, 372.
- (2) Kahlweit, M.; Busse, G. *J. Chem. Phys.* **1989**, *15*, 1339.
- (3) Chen, L.-J.; Jeng, J.-F.; Robert, M.; Shukla, K. P. *Phys. Rev. A* **1990**, *42*, 4716.
- (4) Bonkhoff, K.; Hirtz, A.; Findenegg, G. H. *Physica A* **1991**, *172*, 174.
- (5) Aratono, M.; Kahlweit, M. *J. Chem. Phys.* **1991**, *95*, 8578.
- (6) Chen, L.-J.; Yan, W.-J. *J. Chem. Phys.* **1993**, *98*, 4830.
- (7) Chen, L.-J.; Yan, W.-J.; Hsu, M.-C.; Tyan, D.-L. *J. Phys. Chem.* **1994**, *98*, 1910.
- (8) Chen, L.-J.; Lin, S.-Y.; Xyu, J.-W. *J. Chem. Phys.* **1996**, *101*, 225.
- (9) Kahlweit, M.; Busse, G. *J. Phys. Chem. B* **2000**, *104*, 4939.
- (10) Chen, L.-J.; Chiu, C.-D.; Shau, F.-S.; Cheng, W.-J.; Wu, J.-G. *J. Phys. Chem. B* **2002**, *106*, 12782.
- (11) Hirtz, A.; Bonkhoff, K.; Findenegg, G. H. *Adv. Colloid Interface Sci.* **1993**, *44*, 241.
- (12) Chen, L.-J.; Hsu, M.-C. *J. Chem. Phys.* **1992**, *97*, 690.
- (13) Chen, L.-J.; Hsu, M.-C.; Lin, S.-T.; Yang, S.-Y. *J. Phys. Chem.* **1995**, *99*, 4687.
- (14) Donahue, D. J.; Bartell, F. E. *J. Phys. Chem.* **1952**, *56*, 480.
- (15) Strey, R. *Ber. Bunsen-Ges. Phys. Chem.* **1996**, *100*, 182.
- (16) Cahn, J. W. *J. Chem. Phys.* **1977**, *66*, 3667.
- (17) Aratono, M.; Toyomasu, T.; Shinoda, T.; Ikeda, N.; Takiue, T. *Langmuir* **1997**, *13*, 2158.
- (18) Toyomasu, T.; Takiue, T.; Ikeda, N.; Aratono, M. *Langmuir* **1998**, *14*, 7313.
- (19) Yeh, M.-C.; Chen, L.-J.; Lin, S.-Y.; Hsu, C.-T. *J. Chin. Inst. Chem. Engrs.* **2001**, *32*, 109.
- (20) Stephenson, R.; Stuart, J.; Tabak, M. *J. Chem. Eng. Data* **1984**, *29*, 287.
- (21) Jones, D. C. *J. Chem. Soc.* **1929**, 799–813.
- (22) Pai, Y.-H.; Chen, L.-J. *Fluid Phase Equilib.* **1999**, *155*, 95.
- (23) Lai, H.-H.; Chen, L.-J. *J. Chem. Eng. Data* **1999**, *44*, 251.
- (24) Villers, D.; Platen, J. K. *J. Phys. Chem.* **1988**, *92*, 4023.
- (25) Chiou, D.-R.; Chen, L.-J. *Fluid Phase Equilib.* **2004**, *218*, 229.